

## **EFFECT OF MANUFACTURING METHODS ON THE DECAY OF CERAMIC MATERIALS: A CASE STUDY OF BRICKS IN MODERN ARCHITECTURE OF MADRID (SPAIN)**

Elena Mercedes Perez-Monserrat<sup>a\*</sup>, Fernando Agua<sup>b</sup>, Rafael Fort<sup>a</sup>, Monica Alvarez de Buergo<sup>a</sup>, Juan Felix Conde<sup>b</sup>, Manuel Garcia-Heras<sup>b</sup>

<sup>a</sup> Instituto de Geociencias IGEO (CSIC, UCM) C/José Antonio Nováis 12. 28040 Madrid, España  
empmon@geo.ucm.es, rafael.fort@csic.es, monica.alvarez@csic.es

<sup>b</sup> Instituto de Historia (CCHS-CSIC) C/Albasanz 26-28. 28037 Madrid, España  
fernando.agua@cchs.csic.es, juanfelix.conde@cchs.csic.es, manuel.gheras@cchs.csic.es

Corresponding author:

Elena Mercedes Perez-Monserrat

empmon@geo.ucm.es

Instituto de Geociencias IGEO (CSIC, UCM)

C/José Antonio Nováis 12. 28040 Madrid, Spain

Tlf. 0034 - 913944903

## **Abstract**

The appearance and main decay forms in the fair-faced brick façades on the University Campus of Madrid's Faculty of Medicine were taken as a starting point to analyse certain building's construction characteristics and the clay and technology used in brick manufacture. The raw materials consisted in a mix of Miocene marl and red Triassic clays from the Spanish province of Jaén. The exposed face of bricks was characterised by a yellowish tone and smooth, uniform texture that afforded perfect dimensioning and inter-brick alignment. In some bricks this texture was lost, with a concomitant colour change, surface roughness increase and loss of material. Laboratory studies through polarised optical microscope (POM), X-ray diffraction (XRD) and field emission scanning electron microscopy with energy dispersive X-ray spectroscopy (FESEM-EDS) revealed similar composition in all the bricks, firing temperatures ranging between 800-850°C and, with the exception of the exposed surface, not particularly careful manufactured.

**Keywords:** clays, bricks, built Heritage, preventive conservation, non-destructive techniques (NDT)

## 1. Introduction

The history of brick dates back to the dawn of civilisation (Campell, 2005). Moulded adobe was developed in Mesopotamia around 5000 BC, while with the invention of fired brick around 3500 BC longer lasting structures could be built. The Greeks used fired bricks under the influence of Egypt and Mesopotamia; Rome and Byzantium inherited the Greek aesthetic, from where it travelled to the Far East. The Islamic version reached the Iberian Peninsula after crossing northern Africa. By the early thirteenth century AD brick was found in the rest of Europe, where its use largely conditioned construction progress between the Renaissance and the seventeenth century and where, as a relatively inexpensive material, it pervaded all layers of society. The eighteenth century brought techniques for its large-scale production and shipment across long distances. In the nineteenth and well into the twentieth century it became the standard material for industry and trade. Thereafter brick output gradually rose with the introduction of a wide variety of products and techniques able to support more innovative usage.

In Spain, the ceramic industry and the legacy of traditional manufacturing procedures with a strong Arabic influence are especially significant, primarily due to the abundance of raw materials and centuries old trade relations with other Mediterranean cultures. While ceramic production areas are to be found all across the country, their presence is particularly significant in the provinces of Valencia, Toledo, Jaén, Madrid, Teruel, Castellón and Seville. Adell (1992) noted that enormous technological progress took place in the nineteenth century, when brick began to acquire importance of its own, adopting the industrialised procedures characteristic of the age. Modulation and industrialised manufacturing led to the development of different types of brick (such as hollow, perforated or pressed). As a building material, brick played an essential role in nineteenth-century modernity. Moreover, in that century brick began to be sized to a length approximately double the width, giving rise to bonds with alternating length and width that could not be accommodated with the previous proportions (Adell, 1992; Rodríguez, 2007). Until that time, header (or Spanish) bonds prevailed in Spanish architecture. In Madrid, nineteenth-century brick architecture was characterised by header bonds to attain the maximum possible number of joints, yielding highly subdivided wall surfaces.

When clay is fired changes take place in its mineralogy that depend essentially on the initial composition, kiln temperature, heating rate, firing time and whether oxidising or reducing reactions predominate (Fort et al., 2004; Maggetti, 1982; Maritan et al., 2006). Similarly, the manufacturing procedures and technologies used in ceramic materials have a decisive effect on time-induced decay (López-Arce et al. 2013). The low thermal conductivity of clay translates into temperature gradients between brick surfaces and interiors during firing (Kingery et al., 1976). Brick colour, in turn, is indicative of the composition of the clay used in its manufacture, in particular the amount of iron oxide present and the degree of oxidation (Kreimeyer, 1987).

The many factors involved in the behaviour and alteration of the construction materials comprising Heritage structures must be taken into consideration when characterising and studying the types of decay present. For ceramic materials, that entails identifying the kind of clay used as a raw material, as well as manufacturing technologies and construction methods. The researcher's tools for such studies include documentary sources, observation of the target materials and in-situ and laboratory characterisation techniques. To address this information as a whole allows understanding the brick processing and its

decay, providing the background needed to propose measures for preventive conservation and/or to retard alteration (Perez-Monserrat et al., 2013b).

The primary aim of this study consists in analysing how clay type, brick manufacturing procedures and the construction system used have conditioned the decay of the exposed face of the façade brick on the Faculty of Medicine, University Campus of Madrid (Spain). Guidelines can thereby be established for minimising decay and manufacturing new brick if some units need to be replaced.

#### 1.1. The Faculty of Medicine within the medical ensemble of the University Campus of Madrid (Spain): overall and façade design

In 1927, King Alfonso XIII established a new university campus where faculties and technical schools could be clustered and modernised. The campus was to initially house, among others, the Faculties of Medicine, Pharmacy and Dentistry, all flanking the same square, and a university hospital to be built on a nearby hill (Figure 1). This campus was the origin of the current Complutense University of Madrid (UCM). The Faculty of Medicine, designed by Miguel de los Santos Nicolás, was built between 1930 and 1935. This large-scale, complex design was influenced by the architecture prevailing in U.S. universities and the League of Nations headquarters at Geneva (Switzerland). The building was severely damaged during the Spanish Civil War (1936-1939) and reconstructed in 1941-45. The upper terraces were rebuilt in 1956 and in 1977 the property was listed as a Cultural Heritage asset (Chías, 1986; VVAA, 2003).

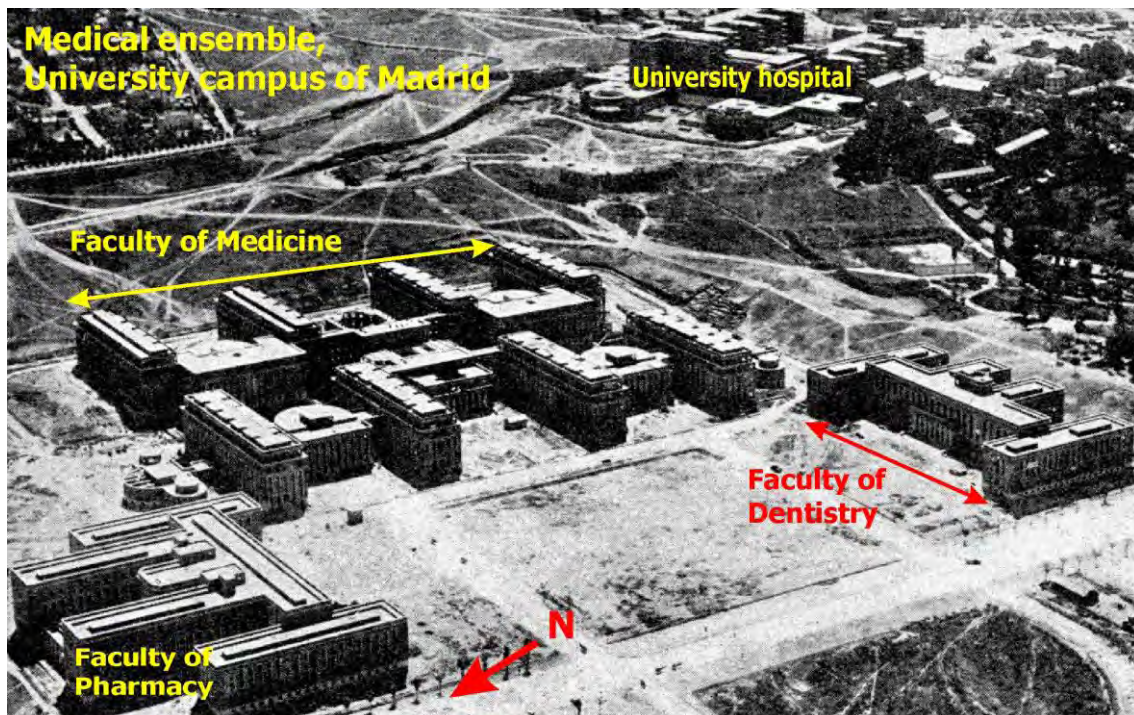


Figure 1. Overview of the buildings that comprise the Medical Ensemble of the current Complutense University of Madrid (Spain) ca 1935.

The building features a reinforced concrete structure, stone materials are used for the socle, impost and mouldings, and fair-faced brick closes the façade. The simplicity, uniformity and rationality of the façade design were informed by principles of economy and functionality. Vertically, it is symmetrically divided into alternating panels and openings, and horizontally into three distinct components: a tall socle, the main (with four-storey bodies) and a setback attic with a terrace. The fourth storey and attic have on its upper part parapets, resting on a cantilevered impost and capped by a narrow ledge (Figure 2b) which is only slightly cantilevered and has no dripstone. In some areas, the fourth-storey parapet sealing has recently been replaced with asphaltic material.

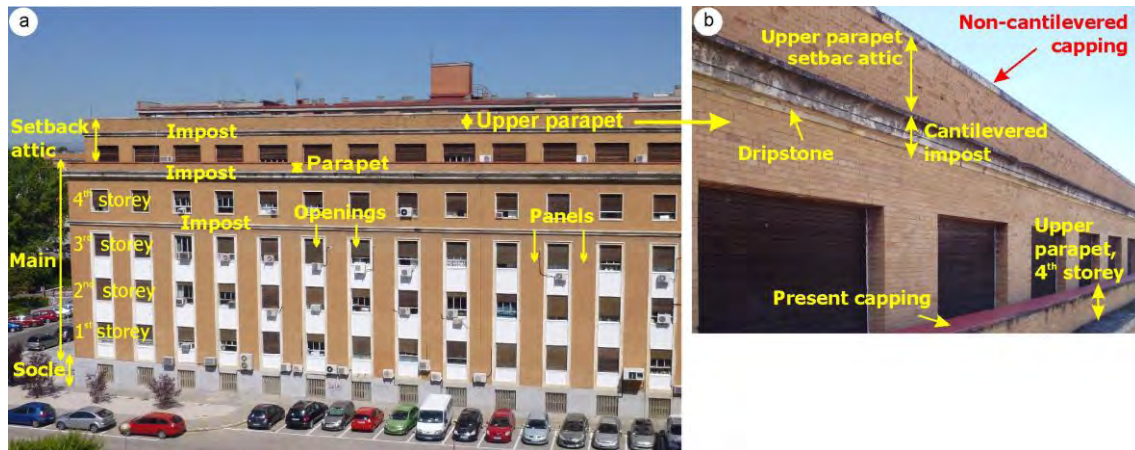


Figure 2. Faculty of Medicine façade design.

a) three main components (from bottom up): socle, main body (4 storeys) and setback attic with terrace. b) detail of setback attic: the narrow ledge capping the upper parapet and the cantilevered cornice-like impost, fitted with a dripstone, can be shown.

## 2. Materials and methods

### 2.1. Methodology and sampling

Three types of studies were conducted: a review of historical documents, bricks examination on façades and in-situ and laboratory characterisation of the bricks.

Information on the construction and reconstruction of the Faculty of Medicine and over building materials provenance was found in the University Campus of Madrid's General Archives (AGUCM). The information on the source of the clay used to manufacture the brick was contrasted with the respective national geological maps (MAGNA, scale 1:50 000). Secondly, brick bond, colour and decay were observed in-situ.

In-situ testing included the measure of bricks dimensions as well as their surface colour and moisture with spectrophotometric and hygrometric techniques, respectively. Brick measurements were taken in three areas (Figure 3): the façades facing west, to the right (area 1) and left (area 2) of the main entrance, and the north setback attic (area 3, probably reconstructed) on the right wing of the building. In-situ measurements were carried out on 39 bricks, with colours representative of all the bricks in each area, and were numbered from 1 to 39 (14 in area 1, 11 in area 2 and 14 in area 3).





Figure 3. Areas selected on the façades for in-situ measurements (areas 1, 2 and 3) or sampling (areas 1, 2, 3 and 4). Details showing the 39 bricks measured (numbered from 1 to 39, in yellow) and the samples taken (No.1 to No.13, in blue, red or green), mostly from the same 39 bricks.

On these 39 bricks, or others with a similar colour, 13 samples were taken, labelled No.1 to No.13. The south end of the parapet crowning the main entrance was also sampled (area 4). Laboratory characterisation of the bricks included macroscopic examinations of hand samples and thin sections, as well as petrographic, mineralogical, microstructural and elemental composition analyses (Table 1), respectively with polarised optical microscopy (POM), X-ray diffraction (XRD) and field emission scanning electron microscopy coupled with energy dispersive X-ray spectroscopy (FESEM-EDS).

Table 1. Brick sampling and in-situ and laboratory characterisation.

	In-situ measurements				Laboratory studies				
	Bricks <sup>(1)</sup>	D <sup>3</sup>	Colour	Moisture	Samples taken	Macroscopic observation	POM	XRD	FESEM-EDS
AREA 1	[1-14]	X	X	X					
	2	X	X	X	No.1	X	X	X	
	4	X	X	X	No.2 <sup>(2)</sup>	X	X	X	
	5	X	X	X	No.4 <sup>(2)</sup>	X		X	
AREA 2	12	X	X	X	No.3	X		X	
	[1-11]	X	X	X					
	2	X	X	X	No.5	X	X	X	
	3	X	X	X	No.6 <sup>(2)</sup>	X	X	X	
AREA 3	9	X	X	X	No.7	X	X	X	
	[1-14]	X	X	X					
	2	X	X	X	No.8	X		X	
	4	X	X	X	No.9	X	X	X	X
AREA 4	8	X	X	X	No.11 <sup>(2)</sup>	X	X	X	X
	12	X	X	X	No.10	X		X	
AREA 4	-	-	-	-	No.12	X	X(outer/inner)	X	
	-	-	-	-	No.13	X	X(outer/inner)	X	X(outer/inner)

(1) Numbering as in yellow in Figure 3 for areas 1, 2 and 3 (bricks 1-39).

(2) Samples taken from pieces with hue similar to the colour of the bricks measured in situ (No.1-No.13).

## 2.2. Characterisation techniques

Brick surface colour was determined by means of Spectrophotometric, non-destructive technique (NDT), with the Geosciences Institute (IGEO) Petrophysics Laboratory's portable MINOLTA CM 700d spectrophotometer fitted with Color DATA SPECTRAMAGIC TM NX CM-S100W software. A D65 standard light source and 10° viewing angle were used to analyse the CIELAB (1978) parameters: lightness ( $L^*$ ), with values ranging from 0 (pure black) to 100 (pure white); chromatic coordinates  $a^*$  and  $b^*$ , which denote hue (greenness/redness ( $-a^*/a^*$ ) and blueness/yellowness ( $-b^*/b^*$ ); and chroma ( $C^*$ ) or colour saturation, indicating colour vividness or dullness, calculated from the formula  $C^*=[(a^*)^2 + (b^*)^2]^{1/2}$ . Ten readings were taken on the exposed face of each of the 39 bricks measured.

Brick surface moisture was determined by a PROTIMETER SURVEYMASTER portable hygrometer belonging to the Geosciences Institute (IGEO) Petrophysics Laboratory. This instrument measures the wood moisture equivalent (WME) in a range of 6-100% to a depth of approximately 25 mm. While initially designed for timber and derivatives, the technique is now widely used for other building materials, yielding proportional values (Gomez-Heras et al., 2014; Aly et al., 2015). Three readings were taken on the exposed face of each of the 39 bricks selected.

An OLYMPUS BX51 transmitted light polarised optical microscope fitted with an OLYMPUS DP12 digital camera was used for petrographic characterisation. These instruments belong to the Petrology and Geochemical Department of the UCM's Faculty of Geology. The technique provides information on ceramic manufacture processes, such as the additives used or the degree of clay vitrification, and the associated decay mechanisms (Ingham, 2013). Thin sections (with a thickness of approximately 30  $\mu\text{m}$ ) taken from the seven largest of the thirteen samples taken were partially stained with alizarin red (Friedman, 1959) to identify carbonates.

The mineral phases identified with XRD mineralogical analysis afford fairly accurate information on firing temperature of ceramic materials. The 13 samples were ground in an agate mortar to a size of approximately 50  $\mu\text{m}$ . Diffractograms were recorded continuously at  $2\theta$  angles of 2-68°, scan step size 0.02° in 2°/min scanning rate on the entire sample, using the IGEO (CSIC-UCM) Microscopy and Mineralogy Technical Unit's PHILIPS ANALYTICAL PW 1752 Cu  $K\alpha$  radiation power diffractometer fitted with a copper anode tube, graphite monochromator and PC-ADP DIFFRACTION software and operating at 40 kV and 30 mA.

Sample microstructure, microtexture and elemental composition were determined with the HITACHI S4800 FEM equipment of the National Centre for Metallurgical Research, Spanish National Research Council (CENIM-CSIC). This instrument operates at an accelerating voltage of 0.5-30 kV, an extraction voltage of 0-6.5 kV and a resolution of 1 nm at a working distance of 4 mm and a working voltage of 15 kV. The samples were observed on polished thin sections and on fresh fractures, sputter-coated with graphite on a JEOL JEE4b vaporiser to make conductive samples. Images were acquired by secondary and back-scattered electron modes at acceleration of 15 kV. Area and point analyses were conducted to establish the qualitative and semi-quantitative elemental composition of the samples and the elements deemed to be of interest were mapped. The Oxford X-Max EDS 20 mm<sup>2</sup> microanalyser attached to the microscope features a rated resolution of 125 eV (Mg  $K\alpha$ ) and a 90 second run time was used.

### 3. Results and discussion

#### 3.1. Documentary study

##### 3.1.1. *Provenance of stone materials*

The builders' modular and systematic construction method deployed to lower costs was likewise applied to the choice of the materials. According to the documents reviewed, both the socle and the stairway and columns at the entrance were made of greyish granite quarried from Ávila and Zarzalejo, northwest of the city of Madrid (AGUCM, 1928). Known as *piedra berroqueña*, this high-quality and durable granite was traditionally used in the region of Madrid (Fort et al., 2013; Freire-Lista and Fort, in press; Perez-Monserrat et al., 2013a). The impostes and the frames around the openings in the main body (storeys 1-4) were made of calcarenite quarried at Almorquí, in the Spanish province of Alicante (AGUCM, 1928). This material, termed as *piedra de Novelda* or *piedra Bateig*, began to be used intensely in the city of Madrid in the mid-nineteenth century when the advent of the railroad lowered shipping costs (Fort et al., 2002).

##### 3.1.2. *Exposed brick and selection of clay raw material: clays from Bailén, Jaén (Spain)*

As noted in section 1.1, the façade enclosures were made of exposed brick. The original design specifications pointed out that outer walls with no stone cladding were comprised of three layers: external one made of thin brick, an intermediate cork layer of 2.5 cm in thickness and an inner one of ceramic brick of 10 cm thick. These three layers were tied together every fourth course with galvanised iron cramps and the brickwork was pointed on the inside with a four-to-one lime and cement mortar (AGUCM, 1928).

Likewise according to the UCM's General Archive, the original intention was to use bricks from nearby Alcalá de Henares (AGUCM, 1931), which had a thriving brick industry (Puche and Mazadiego, 2002). These bricks were ruled out, however, for their insufficient freeze-thaw resistance. Other bricks made with clay from towns around 200 km northwest of Madrid likewise failed the freeze-thaw test, so they were also discarded.

Ultimately the bricks for the Faculty of Medicine (and of Pharmacy and Dentistry) were supplied by Ilturgi, S.A., a company working out of Andújar, an Andalusian town close to Bailén in the Spanish province of Jaén. A prominent manufacturer from the mid-nineteenth through the mid-twentieth century, Ilturgi closed in 1960. According to an order dated 28 January 1932, the company committed to supplying one million bricks and more if needed. The agreement concluded with the company stressed the importance of brick colour uniformity, specifying that if the site supervisor rejected a batch of bricks on the grounds of colour mismatches, 15% would be kept for the works and the rest returned to the supplier.

The documents reviewed refer back to the geological substrate underlying Bailén, where the local ceramic industry quarried Tertiary (Miocene) marl clays lying in the Guadalquivir Depression and the red Triassic clays that blanket the Iberian Massif (IGME, 1977, 2013) (Figure 4). Galán-Arboledas et al. (2013) noted that these Miocene marl clays comprise so-called white, yellow and black clay. All three are quartz-, calcite-, illite- and smectite-high and contain as well some foraminifers, especially globigerines (marine



microfossils). The red Triassic clays contain fragments of slate and dolomite, barely any calcite, some kaolinite and high concentrations of illite.

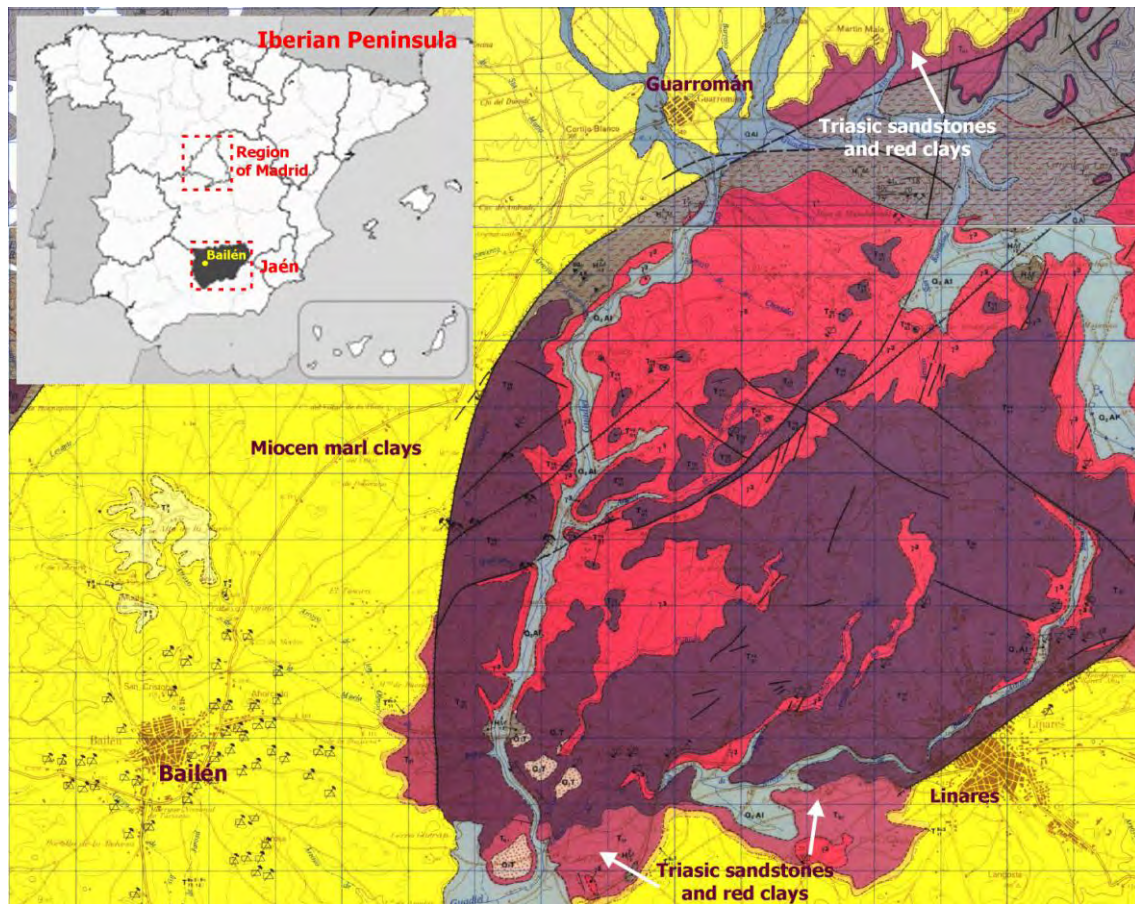


Figure 4. Location of the Spanish provinces of Madrid and Jaén and geological map of Bailén surrounding area.

Clay materials used to manufacture the bricks analysed: Miocene marl clays underlying the town of Bailén and surrounds and red Triassic clays found around Linares and Guarromán (MAGNAS, Nos. 885 and 905).

Its high smectite content affords Miocene clays medium-high plasticity, with the concomitant drying problems. As kaolinite lowers clay plasticity, materials containing this mineral exhibit excellent drying properties (Melgarejo, 2003). Neither the white Miocene nor the red Triassic clays are apt for brick production alone but must be mixed, for their plasticity values lay outside the optimal 15-25% H<sub>2</sub>O content range recommended for extrusion (González et al., 1998; Vázquez and Jiménez-Millán, 2005).

### 3.2. Description of brick façades

#### 3.2.1. *Bonds and appearance*

The thin bricks referred in the original design specifications enclosed the panels in the main body façades (Figures 2a and 5a). These units were 3 cm in thickness and were dry laid to header bonds (Figure 5a), header and stretcher bonds (at the corners) or irregular stretcher and header bonds where at the contact area with the stone frames around the openings (see detail, areas 1 and 3, Figure 3). Due to the absence of mortar in the outer joints the bricks had to be manufactured to engage perfectly with one another: hence the very smooth and carefully dimensioned exposed faces.

The partial loss of some units of the setback attic, especially in the parapet that crowned the building, showed that brick was not a cladding element in that area. It dealt with a brick fabric comprised of compact box and H-shaped bricks laid to a block bond and filled inside with mortar (Figure 5b). The bricks apparently played a certain structural role, although as they were positioned high on the façades they bore fairly light loads. Their exposed face was also observed to be smooth and precisely dimensioned and as in the main body, they were laid to a header bond except at plane intersections, where likewise stretcher and header bonds were used.

The bricks were found to exhibit two main hues, yellowish and brown, although the former predominated (Figure 5a). Examination showed that most of the yellow bricks had a smooth and uniform surface (1 in Figure 5a), although a few exhibited a rougher and less uniform surface, a darker colour and a profusion of aggregate inclusions (2 in Figure 5a). The brown bricks, distributed randomly on the façades, had rough surfaces in general as well as a profusion of aggregates (3 in Figure 5a). Many smooth yellowish bricks in particular but others also, were observed to have a reddish hue, although not across the entire exposed face (5 in Figure 5a). This gradient toward reddish hues was found in some of the rough brown bricks as well, although there the change in colour was less perceptible. An occasional smooth textured off-white or pale grey brick was also observed (6 in Figure 5a).

Most of the bricks in the walls underneath the parapets that crown the setback attics were likewise found to be yellowish, paler and very smoother and more uniform surface at lower courses (Figure 5c). Observations showed that all the bricks had certain degree of gloss, which was much more visible on the setback attics. In conjunction with the smooth and uniform texture of the latter, that gloss may denote surface grinding or be the result of the extrusion procedures used. Details of some of the bricks measured or sampled in areas 1, 2 and 3 are displayed on the second and third rows of photographs in Figure 5 (the bricks measured in-situ and the samples are numbered as shown in Figure 3).

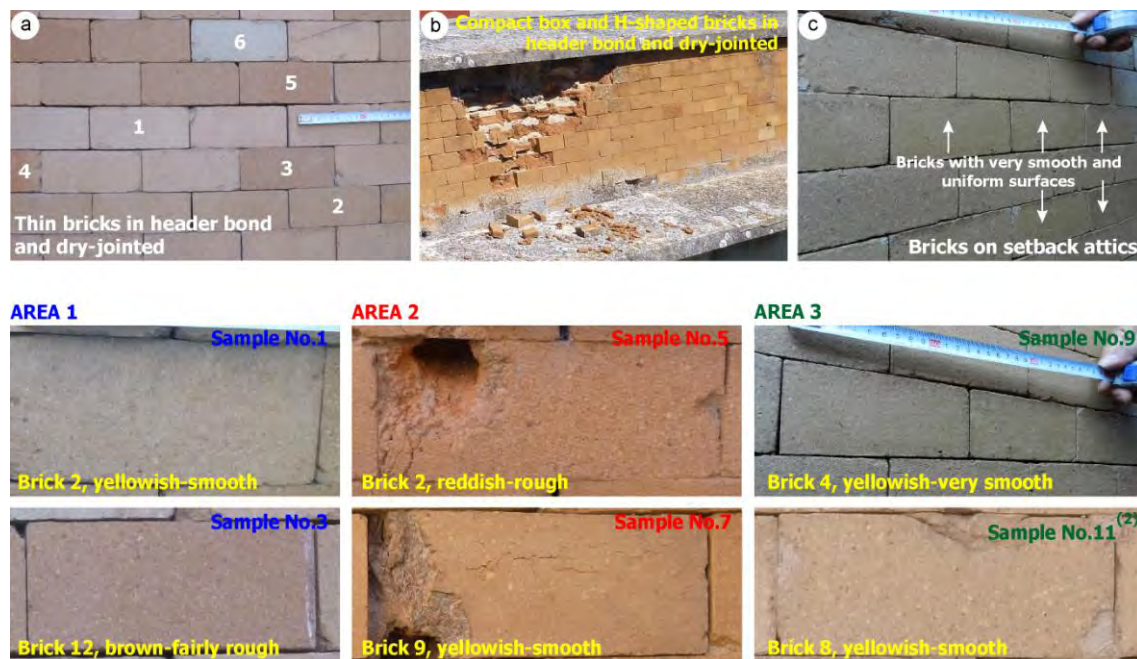


Figure 5. Brick bonds and appearance (colour and texture).



- a) thin bricks in main body façade enclosures: (1) yellowish and smooth surfaces; (2) dark yellow and rough; (3) dark brown; (4) yellowish, partly reddish, smooth; (5) off-white or light grey and smooth surface.
- b) brickwork on upper attic parapet: joint mortar pointing on the inside as well as the lower cantilevered cornice and the non-cantilevered capping can be shown.
- c) dry-jointed brick in setback attic: the very smooth and uniform yellowish surface on some of the bricks is displayed.
- Areas 1, 2 and 3: surface hue and texture of some of the bricks selected for in-situ measurements and sampling (numbering and colour code as in Figure 3).

### 3.2.2. Conservation state of the bricks

The bricks were in good condition, generally speaking, thanks primarily to the city of Madrid's dry climate (continental Mediterranean as per the Köppen classification), the building's location in an area of the city with low levels of air pollution and to its relatively recent construction (1930-1935) and subsequent interventions (1941-45 and around 1956).

Although most of the bricks were observed to exhibit a yellowish hue and uniform texture on the exposed face, two forms of generalised decay were also found in many. The first, surface colour change, particularly in units located at plane intersections or at the interface with the stone around openings (especially on stretchers), consists in a turn from yellowish to reddish hues (many fewer brown bricks had turned reddish) and was attendant upon a gradual change from a smooth, uniform surface to a rough uneven surface with aggregate inclusions (Figure 6a).

In the setback attic, the very smooth, uniform and yellowish bricks underneath the parapet, especially the ones in the lower courses, exhibited barely any colour or textural change (Figure 5c). The exception was the alternating stretchers at the corners (Figure 6b).

Many of the units on the parapet over the setback attics were found to exhibit surface roughness and cracks, often with scaling. In addition to the concomitant loss of material, this situation constituted a hazard due to possible fragment detachments. This decay was directly related to brick exposure to rainwater at this high elevation, for the scantily cantilevered capping and the absence of a dripstone (Figure 2b) leave the material essentially unprotected (Figure 6c). Fragment loss had also led to some degree of colour variation in this area of the setback attics, where the exposed bricks were darker and characterised by crumbling and powdering.

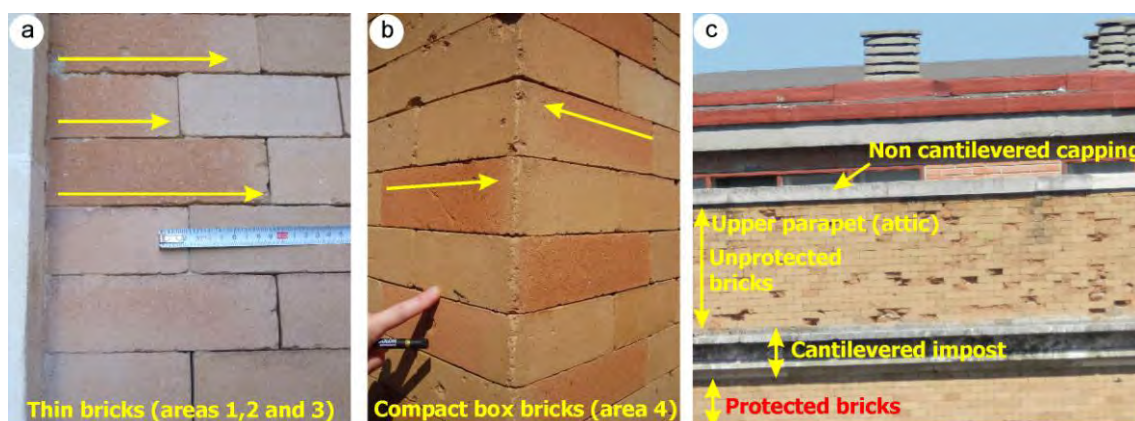


Figure 6. Main forms of decay observed in façade bricks.

- a) gradual colour change and increasing roughness in bricks that interface with the stone framing on openings.
- b) gradual change in surface texture in corner bricks (setback attic).
- c) partial detachment of bricks in the upper brickwork parapet on the setback attic due to the scant protection afforded by the capping, compared to the bricks under and protected by the cantilevered impost.

Many units, especially on the west façades, exhibited a partial loss of material due to the impact of Civil War bullets, while some of the panels had cracked under differential settling. Other forms of decay were occasionally observed, such as the scaling- or cracking-induced loss of brick vertices and arris, cracks running vertically across entire units or slight shifting.

### 3.3. Brick characterisation

#### 3.3.1. *In-situ measurements (areas 1, 2 and 3)*

The dimensions of the 39 bricks chosen are listed in Table 2, along with the mean colour parameters and mean surface moisture and standard deviation for the bricks in each area. The table also specifies whether the exposed face was found to be smooth or rough. In all, 72% of the bricks had a smooth and the remaining 28% a rough surface. Surface roughness was patterned along a gradient in any given brick and inter-brick differences were observed. The overall mean moisture and colour coordinate values are given by surface texture (rough or smooth) in the bottom rows of the Table 2.

The vertical dimension was fairly constant throughout, with a mean value of  $60 \pm 1$  mm. The header varied, however, from 139 to 144 mm in most bricks, with a few outliers ( $>175$  mm or  $<100$  mm). The result is longer or shorter bricks which, as noted in section 3.2.1, were laid more or less irregularly to a stretcher and header bond (detail of areas 1 and 2 in Figure 3). This may have been to strengthen the units or adjust them to the enclosed area by alternating stretchers and headers at the interface with the stone moulding around the openings.

The smooth surfaces exhibited higher lightness values ( $59 \pm 2.4$ ) and lower saturation ( $26 \pm 3.4$ ) than the rough surfaces ( $L^* = 55 \pm 2.4$  and  $C^* = 29 \pm 3.0$ ). The latter, in turn, had somewhat higher mean  $a^*$  and  $b^*$  values than the smooth surfaces ( $a^* = 13.9 \pm 3.2$  and  $b^* = 24.9 \pm 1.7$  versus  $a^* = 10.6 \pm 2.5$  and  $b^* = 23.4 \pm 2.8$ ). The 39 bricks measured were grouped into three chromatic groups on the grounds of their  $a^*$  and  $b^*$  values, as follows:

- Group A:  $5.5 < a^* < 9.2$  //  $16.9 < b^* < 21.7$ ; total bricks: 10 (25.6%), off-white or pale grey
- Group B:  $10 < a^* < 12$  //  $22 < b^* < 28$ ; total bricks: 19 (58.7%), yellowish
- Group C:  $12 < a^* < 17$  //  $25 < b^* < 28$ ; total bricks: 10 (25.7%), brown and reddish

The mean  $a^*$  values are plotted against the mean  $b^*$  values for each brick and the data points are clustered by group A, B or C in Figure 7. Generally speaking, nearly half of the bricks were observed to lie in group B (yellowish) and the bricks in the setback attic (area 3) exhibited higher  $b^*$  values and a narrower scatter. Group A varied more widely in hue, with off-white to light grey tones, and two bricks were excluded. The  $a^*$  values (approximately 10-12) ranged more narrowly than the  $b^*$  values (22-28) in the group B (yellowish) bricks. The group C units exhibited substantial  $a^*$  value variation, leading to a subdivision into  $12 < a^* < 15$  // 10

25<b\*<28 (brown hues) and 15<a\*<17 // 25<b\*<28 (reddish hues, which further to the in-situ observations were found in originally yellowish bricks). Group C (brown and reddish) had more rough than smooth surface bricks, especially in the units with higher a\* values, i.e., bricks with a more reddish hue.

Figure 7 also displays the mean L\*, a\*, b\* and C\* values and standard deviations for each group of bricks. Lightness (L\*) was greatest and saturation (C\*) lowest in the group A bricks (hence their lighter hue) and vice-versa in the group C bricks. The group B bricks followed an intermediate pattern.

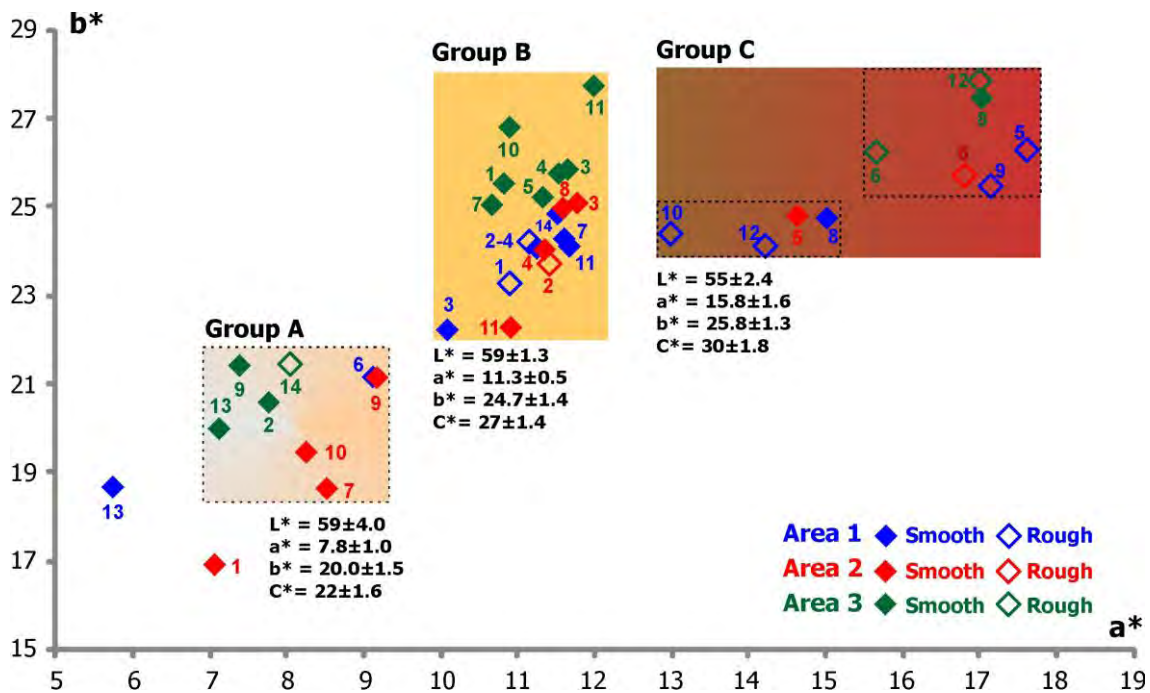


Figure 7. Colour coordinate a\* versus coordinate b\* for the 39 bricks analysed, grouped by hue [group A (off-white, pale grey), group B (yellowish), group C (reddish-brown)] and showing smooth/rough surface texture and area number as well as the mean L\*, a\*, b\* and C\* values and standard deviations for each colour group.

The surface moisture values ranged from 9.9 to 17.9% WME. In areas 1 and 2, the highest moisture (>13% WME) readings were taken in bricks in contact with the stone window frames (5 and 9 in area 1; 6 in area 2) or which had a brown and rough surface (10 and 12 in area 1). In area 3, the surface readings for bricks 5, 6, 7, 12 and 15 were higher than 13% WME and units 6 and 12 exhibited a rough, brown or reddish surface. Bricks 12 and 15 were positioned on a corner.

The mean value was similar for the three areas, ranging from 11.8 to 12.6% WME. The highest and most widely scattered values were found in the setback attic (area 3) (surface moisture = 12.6±2.3). These higher moisture values were primarily attributable to the north orientation of the setback attic selected (Figure 3), where the water absorbed by the fired clay bricks evaporates more slowly. Moisture levels were also found to rise from the lower to the higher courses (12.9 to 15.5), explaining the wider scatter on this façade. The mean for all the rough surface bricks was higher than for the smooth surface units (%WME = 13.7 versus 11.5) (Table 2).

On the grounds of the in-situ observations and measurements, the moisture concentrating at the interface between the bricks and the stone frames around openings and its diffusion across the entire brick can be said to induce the colour change in the exposed face, with the original yellowish hue gradually giving way to a reddish tone (Figure 6a). Attendant upon this process is a gradual rise in roughness, for as the smooth, uniform surface recedes, it exposes the inner body of the brick, which is not only reddish but contains numerous aggregate inclusions and therefore an uneven texture. Therefore, the yellower and consequently smoother surface bricks were less decayed. At plane intersections, either between the panels and the openings lacking stone moulding (area 3, setback attic) or at corners, brick decay was attributable to the same process, although in these areas moisture diffuses primarily from the joint with the adjacent bricks (Figure 6b).



Table 2. Dimensions, mean and standard deviation surface moisture and colour parameters measured in situ bricks (1-39).

Bricks <sup>(1)</sup>	Surface texture	DIMENSIONS (mm)		MOISTURE (%WME)		COLOUR PARAMETERS				
		Vertical	Header	Piece	Area	L*	a*	b*	C*	
AREA 1	1	Rough	60	142	12.1±0.2	11.8 ± 1.3	59±1.0	10.9±0.4	23.3±0.7	26±0.8
	2	Rough	60	142	10.9±0.4		57±1.7	11.1±0.3	24.3±0.5	27±0.5
	3	Smooth	60	142	11.4±0.2		60±0.7	10.1±0.2	22.3±0.4	25±0.4
	4	Smooth	59	142	10.9±0.0		58±0.5	11.2±0.4	24.1±0.5	27±0.6
	5	Rough	58	185*	13.3±0.6		55±1.0	17.6±0.4	26.3±0.9	32±0.9
	6	Smooth	57	142	10.5±0.1		62±1.2	9.1±0.2	21.2±0.4	23±0.4
	7	Smooth	59	139	11.6±0.6		57±0.8	11.6±0.3	24.3±0.9	27±0.9
	8	Smooth	61	184*	11.2±0.0		58±1.3	15.0±2.1	24.8±0.9	29±1.8
	9	Rough	60	184*	14.0±0.8		52±1.1	17.1±2.3	25.5±1.3	31±2.2
	10	Rough	60	141	13.3±0.8		54±1.4	13.0±0.5	24.5±0.5	28±0.5
	11	Smooth	61	141	10.7±0.4		60±0.6	11.7±0.3	24.2±0.6	27±0.7
	12	Rough	61	141	13.8±0.2		52±1.1	14.2±0.9	24.2±1.1	28±1.4
	13	Smooth	61	141	10.5±0.4		62±0.7	5.7±0.4	18.7±0.5	20±0.6
	14	Smooth	61	141	11.2±0.2		59±1.1	11.5±0.3	24.9±0.4	28±0.4
AREA 2	1	Smooth	60	141	11.2±0.1	12.0 ± 0.9	57±1.3	7.1±0.5	17.0±1.1	18±1.2
	2	Rough	61	142	12.0±0.7		58±1.0	11.4±0.4	23.8±0.9	26±1.0
	3	Smooth	60	141	12.5±0.3		58±0.7	11.8±0.2	25.1±0.5	28±0.5
	4	Smooth	60	98*	12.7±0.3		58±1.9	11.3±0.2	24.1±0.6	27±0.6
	5	Smooth	61	177*	12.2±0.4		59±1.0	14.6±2.1	24.9±0.9	29±1.7
	6	Rough	58	177*	13.2±0.5		55±1.0	16.8±0.9	25.8±0.9	31±1.3
	7	Smooth	60	141	11.1±0.3		57±1.2	8.5±0.3	18.7±0.8	21±0.9
	8	Smooth	60	140	13.0±0.3		58±0.7	11.6±0.2	25.1±0.4	28±0.4
	9	Smooth	60	144	11.0±0.2		58±1.2	9.2±1.0	21.2±1.8	23±2.0
	10	Smooth	61	141	10.6±0.2		57±0.8	8.2±0.5	19.5±0.8	21±0.9
	11	Smooth	59	143	12.3±0.3		58±0.7	10.9±0.2	22.3±0.5	25±0.6
AREA 3	1	Smooth	59	141	12.9±0.0	12.6 ± 2.3	60±1.0	10.8±0.4	25.6±0.6	28±0.7
	2	Smooth	59	140	10.6±0.1		65±2.5	7.8±0.8	20.6±1.0	22±1.1
	3	Smooth	59	140	11.8±0.3		58±0.6	11.6±0.1	25.9±0.2	28±0.2
	4	Smooth	62	142	11.4±0.2		59±0.9	11.5±0.2	25.8±0.7	28±0.7
	5	Smooth	61	140	13.5±0.2		58±1.2	11.3±0.2	25.3±0.5	28±0.4
	6	Rough	60	141	17.9±0.6		52±1.2	15.6±0.7	26.3±1.0	31±1.1
	7	Smooth	61	142	13.6±0.3		58±1.5	10.7±0.4	25.1±0.5	27±0.6
	8	Smooth	58	141	11.5±0.2		56±1.3	17.0±0.6	27.6±0.6	32±0.7
	9	Smooth	59	142	9.6±0.4		65±1.0	7.4±0.5	21.6±0.5	23±0.6
	10	Smooth	59	142	10.4±0.2		63±0.6	10.9±0.4	26.9±0.9	29±0.9
	11	Smooth	59	141	12.5±0.4		59±1.4	12.0±0.4	27.8±0.6	30±0.6
	12	Rough	60	90*	15.4±0.4		53±1.9	17.0±0.5	27.9±0.5	33±0.5
	13	Smooth	60	139	9.9±0.4		54±17.2	7.1±7.4	20.0±7.7	22±9.5
	14	Rough	60	95*	14.9±1.3		55±12.1	8.0±3.3	21.5±5.3	23±5.7
smooth surfaces		-	-	11.5±1.1		59±2.4	10.6±2.5	23.4±2.8	26±3.4	
rough surfaces		-	-	13.7±1.9		55±2.4	13.9±3.2	24.9±1.7	29±3.0	

Mean surface moisture and standard deviation for the bricks in each area and mean moisture and colour values by rough or smooth surface texture are also pointed out.

(1) Numbering as in yellow in Figure 3 for areas 1, 2 and 3.

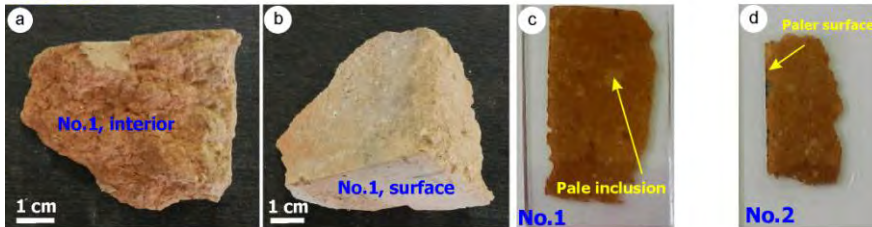
\*Outlier (header range 139 to 144 mm must be taken into account)

### 3.3.2. Laboratory studies and analyses (areas 1 to 4)

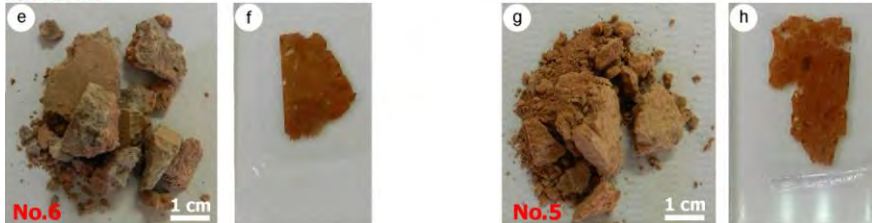
#### 3.3.2.1. Macroscopic observation (hand samples and thin sections)

The brick fragments collected were reddish-brown and somewhat yellow on the surface (Figure 8). The setback attic samples (area 3) were somewhat yellower (Figures 8i and 8k), whereas in the area 4 fragments had a yellowish outer region that could be clearly distinguished from a visibly disaggregated/cracked reddish inner region, generating a more perceptible colour gradient (Figures 8m and 8o). Macroscopic examination of the thin sections revealed sample non-uniformity in terms of the distribution, type and size of aggregate inclusions, particularly visible in samples of the area 4 (Figures 8n and 8p), while the area 3 pieces were more uniform (Figures 8j and 8l). Inclusions of up to 2 mm were observed, some pale and sub-round (Figures 8c and 8d) and others darker and with elongated morphologies. The latter abounded in the area 4 bricks in particular (Figures 8n and 8p). The intense reddish tone in the stained clay matrix in the area 3 pieces (Figures 8j and 8l) denoted the presence of calcium carbonate. The area 4 bricks exhibited the aforementioned colour gradient (Figures 8n and 8p). Besides the lighter coloration to the surface observed in many samples, No.9 sample had a paler surface than interior, but its thin section featured a unique surface layer around 3 mm thick on average that acquired an intense reddish colour when stained (Figure 8j).

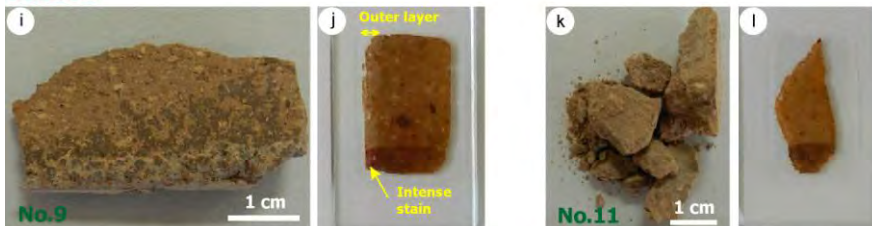
#### AREA 1



#### AREA 2



#### AREA 3



#### AREA 4

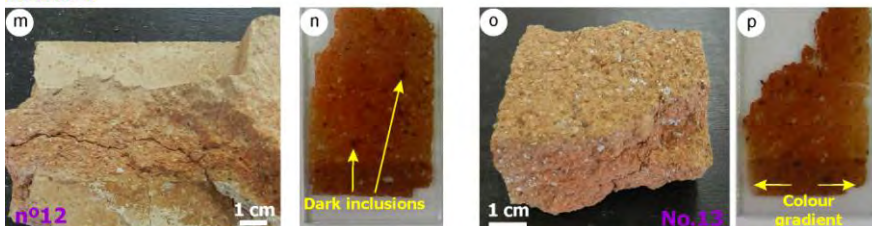


Figure 8. Samples from four areas on the façades and respective thin sections.

### 3.3.2.2. Petrographic analysis

The POM observation of the samples (Figure 9) revealed a profusion of aggregate inclusions in the clay matrix, at a visually estimated aggregate-matrix ratio of 3:1. These aggregate inclusions mainly comprised mono-mineral and sharp-edged quartz grains, perhaps denoting the deliberate inclusion of aggregate additions rather than their natural presence in the clay sediment used. Feldspars, granite and sandstone fragments, as well as foraminifers, primarily globigerines, were likewise observed (Figure 9a). A carbonate-high clay that also contained foraminifers was found in the irregular sub-rounded and pale colour inclusions (Figure 9b). The darker and elongated inclusions were identified to be slate fragments around which shrinking cracks formed, so brick cracking was favoured (Figures 9c and 9d).

Brick surfaces were more uniform and paler in colour than the clay matrix and much smaller inclusions can be observed (Figures 9d, 9f and 9g). Cracking was sometimes observed in the surface (Figure 9f). Quartz aggregate inclusions were occasionally observed to protrude on the surface. A greyish matrix with numerous reddish inclusions, possibly grog or chamotte (Cuomo di Caprio et al., 1993), formed the outer layer observed in sample No.9 (Figure 8j). This layer differed from the surfaces of all the other samples studied and was separated from the underlying clay matrix by a very distinct crack (Figure 9e).

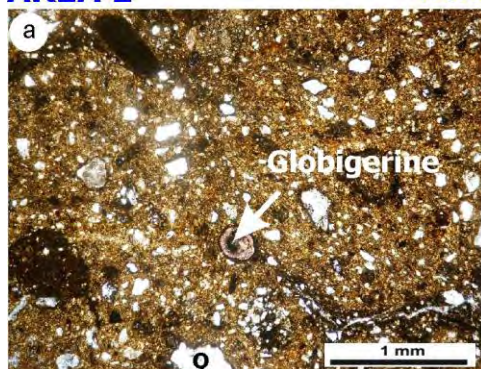
In the area 4 bricks, uniform surfaces prevailed with a lighter colour and smaller sized inclusions than in the underlying material. The clay in this inner part of the bricks was darker and had larger cracks. Slate fragments and possibly grog (Cuomo di Caprio et al., 1993) were identified, surrounded by shrinkage cracks (compare the outer region in Figure 9g to the inner in 9h).

The aforementioned petrographic findings suggest that the bricks may have been made with a mix of clays: a yellow, perhaps a Miocene marl clay containing foraminifers, and a red Triassic clay containing slate fragments. The presence of globigerines in the samples analysed may allow allocating the constituent clay identified as Miocene marl clays extracted at Bailén. Besides, the use of other bricks, initially also selected for the works, can be ruled out, inasmuch as they were manufactured in other areas of Spain where the geological substrate lacks such marine microfossils. Lastly, related to the brick surfaces, the samples collected in areas 1, 2 and 4 had a paler surface and smaller inclusions than the body clay matrix, whereas the surface observed in sample No.9 (area 3) did not appear to consist in a ceramic material.

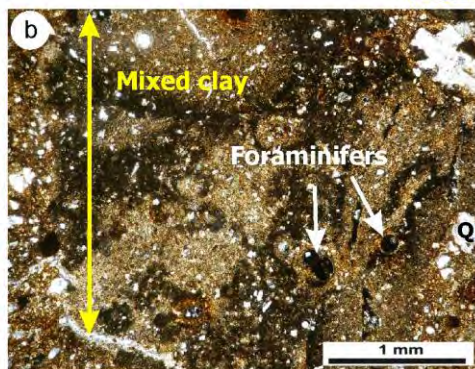


## AREA 1

No.1

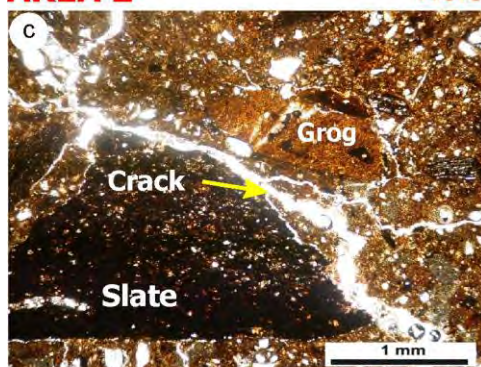


No.2

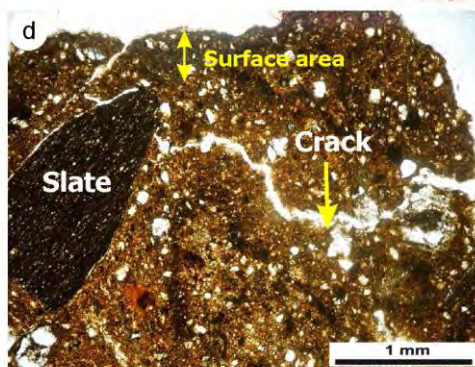


## AREA 2

No.5

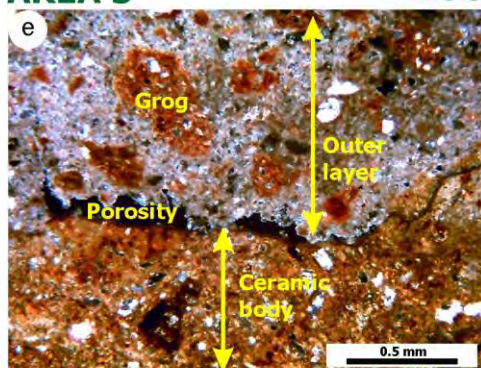


No.6

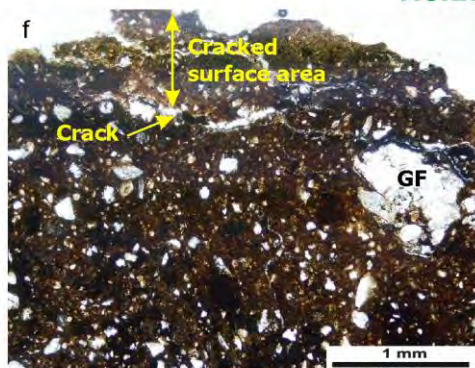


## AREA 3

No.9



No.11

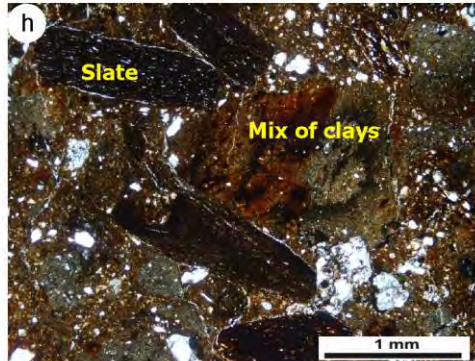


## AREA 4

No.12



No.13



Outer area of brick

Inner area of brick

Figure 9. Polarised optical micrographs of the bricks studied. Crossed nicols in 9e, parallel nicols in rest; Q = quartz; GF = granite fragment.

### 3.3.2.3. Mineralogical composition

The XRD analysis showed that the brick samples studied were mineralogically similar (Figure 10). They were made with similar raw materials and fired at similar temperatures. The main phases identified were quartz, feldspars (orthoclase, albite or both), calcite and illite. Quartz and feldspars were primarily present in the aggregate inclusions observed in the thin sections, whilst the calcite and illite mainly formed part of the clay matrix. Other mineral phases detected included gypsum and hematites. Gehlenite was also identified, with a very faint diffraction line in nearly all the samples and a significant presence in sample No.11 only (Figure 10, area 3). An analysis of sample No.13 (Figure 10, area 4) revealed less intense illite reflections in the outer than in the inner region, a possible indication that the firing temperature was higher on the surface or that during brick extrusion a smaller particle size was chosen for the outer clay, which would contain more illite. As illite has high iron oxide content, the difference in concentration in the two regions would explain the colour gradient observed (Figures 8m to 8p).

Illite becomes fully dehydroxylated at a firing temperature comprised between 800-900°C (Maggetti, 1982), calcite decomposes from 750-800°C depending on its particle size and crystallinity (Shoval et al. 1993) and gehlenite begins to form at around 800°C (Peters and Iberg, 1978); hence the presence of calcite and illite and the incipient formation of gehlenite in the bricks provide grounds for establishing the firing temperature at 800-850°C (Carretero et al., 2002) for most of the bricks analysed. The presence of gehlenite can be associated with clays having certain calcium carbonate content in the form of calcite, since gehlenite is a calcium aluminosilicate formed when the phyllosilicates in clay react with the calcium oxide (CaO) yielded in calcite decomposition (Cultrone et al., 2001; Peters and Iberg, 1978; Trindade et al., 2009). Besides, the significant presence of gehlenite in sample No.11 (Figure 10, area 3) attests to firing temperatures of nearly 900°C in some bricks, probably manufactured from yellow Miocene marl clays.

The detection of hematites, which appear from 700°C in oxidising conditions (Maniatis et al. 1981; Nodari et al. 2007), would in all likelihood be due to the use of iron-rich illitic clay. Although air pollution is low in the area where the Faculty of Medicine is located, the gypsum identified in some of the samples may be related to slight atmospheric SO<sub>2</sub>-induced sulfation on the brick surface (Cultrone et al., 2007).

Since most of the bricks may have been extruded, finer particle clay would have been chosen for the surface, so greater sintering has been favoured and as a result less porosity and a higher surface gloss (Kingery, 1976). The bricks were fired at a temperature of 800-850°C. While not especially high, such temperatures sufficed to sinter non-structural brick apt for cladding and lowered production costs considerably.



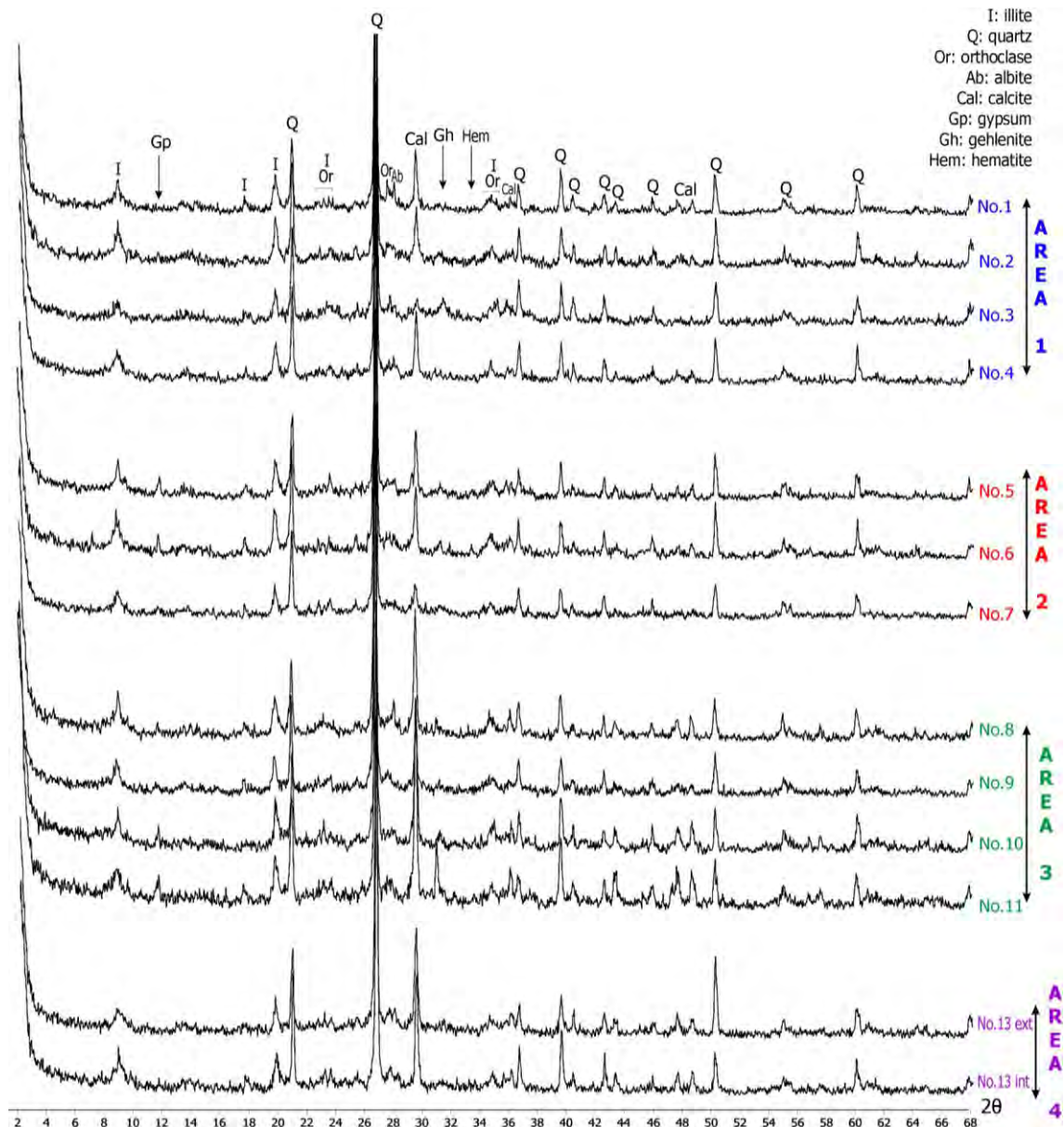


Figure 10. Diffractograms derived from the samples analysed.

#### 3.3.2.4. Microstructure, microtexture and elemental composition

FESEM-EDS techniques were employed to observe the differences between the surface and the underlying body in sample No.9 (Figure 11) with a view to confirming and contrasting the POM and XRD data, in particular those findings connected with the possible existence of a different type of surface layer. In addition to containing grog, this layer was very porous (Figure 11a) and had a calcium oxide content of around 50% according to the analyses conducted. That value is high even for very calcareous clays. The white clay from Bailén, for instance, has a mean 16.6 wt% and a maximum 20-25 wt% calcium oxide content (Galán-Arboledas et al., 2013). At greater magnification, re-carbonated calcite inclusions were identified (Shoval et al., 2003), while EDS microanalysis revealed high calcium, silicon and aluminium



oxide contents in this layer. The microstructure of the underlying ceramic body, in contrast, was characteristic of sintered, non-vitrified ceramic material (Figure 11c), which is consistent with a firing temperature of 800-850°C. The ceramic body exhibited a higher relative silicon and aluminium oxide content and a lower concentration of calcium oxide (~12 wt%) than the outer layer (Figure 11d). Calcium element mapping confirmed its higher concentration in the surface layer and the presence of grog, which contains barely any calcium (Figure 11e).

The FESEM-EDS data showed, then, that this surface layer comprised a lime-based material to which brick grog was added as an aggregate, and that neither the microstructure nor the chemical composition of this layer was the same as found for the ceramic material in the body of the brick.

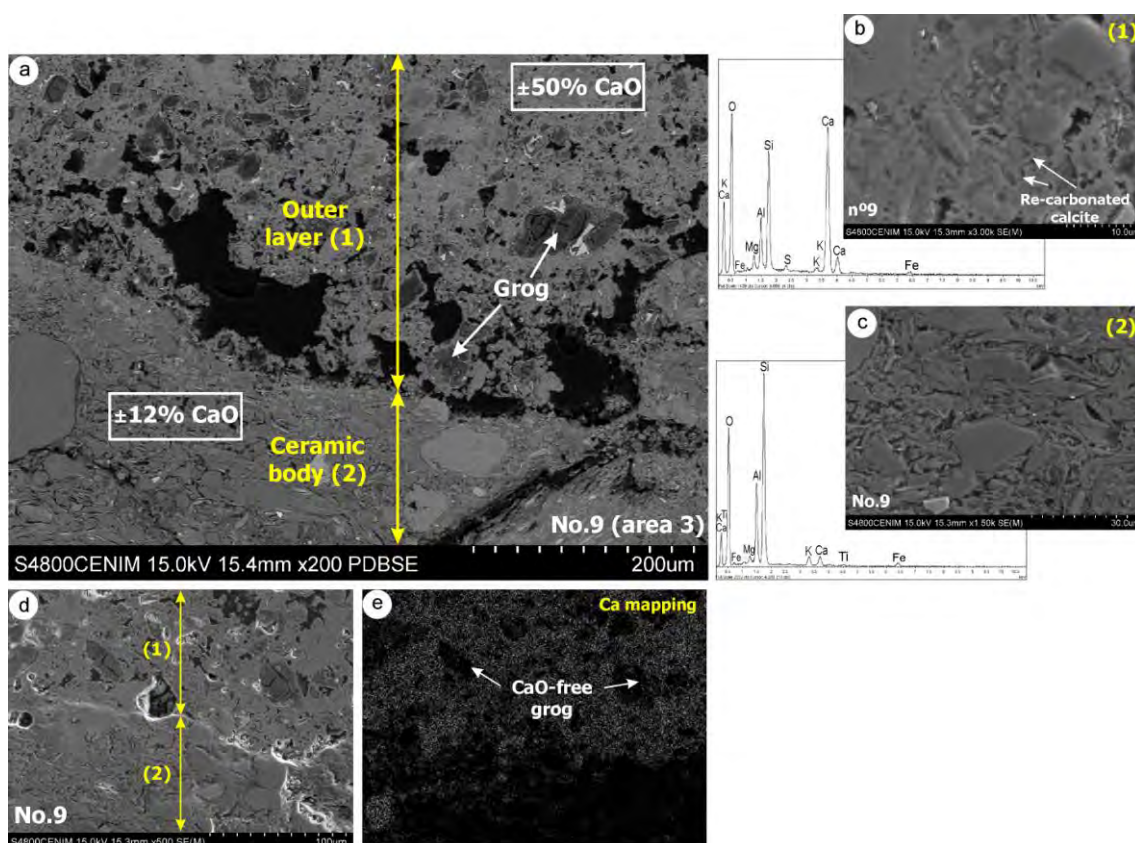


Figure 11. FESEM-EDS microstructure, microtexture and elemental composition of sample No.9 from area 3 (setback attic): a) BSE images; b), c) and d) SE images.

## 4. Conclusions

### 4.1. Brick manufacture

The bricks analysed were made from a mix of yellow Miocene marl clays and red Triassic clays from Bailén, a ceramic production centre in the Spanish province of Jaén. Manufacture was not particularly meticulous as regards either the mix of clays or the choice and distribution of particle size. The bricks were fired at a temperature of 800-850°C. Although not very high, this temperature can be regarded as sufficient to sinter non-structural bricks. The surface clay in most of the bricks was more uniform and paler in colour and had much smaller inclusions than the clay in the body of the bricks. That was very likely attributable to

the extrusion procedures, which selected a smaller particle size clay on the surface to induce greater sintering, lower porosity and a higher gloss. These surfaces, visible on most of the exposed faces, afford the bricks their precision alignment and high freeze-thaw resistance.

The analysed bricks in the setback attic (area 3) were very likely manufactured at a different time or to a different procedure than the pieces in areas 1, 2 and 4. If new bricks were manufactured to rebuild the terraces in 1956, they may well have been made by the original suppliers, a company that was still in business at the time (although it declared bankruptcy in 1960). The study evidences that the bricks in area 3 were made from a clay similar to the raw material used in the other areas, although it was more calcareous and the product was manufactured more uniformly and carefully. The lime-based, grog-bearing material identified on the surface of some of these bricks, those that displays a very smooth and uniform surface, may have been applied intentionally to secure a smooth and uniform surface as well as to afford the material some degree of protection and weatherproofing.

All the bricks may not have originally had a smooth yellow surface, for both brown and yellowish units with a wholly rough surface and no differential decay across the exposed face were found distributed at random on all the façades. In other words, these rough brown or yellowish bricks may have formed part of the 15% retained for use when the site supervisor rejected a lot on the grounds of colour mis-matching.

#### 4.2. Decay

According to the documents reviewed, in the preliminary tests conducted on bricks from various areas of the country, particular importance was attached to the resistance, especially freeze-thaw resistance, requirements to be met by the material once laid. To lower manufacturing costs, the specifications ultimately called for less expensive bricks in which only the surface of the exposed face would be subject to resistance as well as to colour and textural uniformity requirements. The brick decay observed here is directly associated with this circumstance.

As the exposed face of most of the bricks initially exhibited a yellowish hue and a smooth and uniform surface, the façades were initially more homogeneous than at present. The environs and the passing of time have altered the brick surfaces, gradually exposing the underlying body: a mix of unevenly distributed clays containing aggregate inclusions. The fairly speedy and irreversible decay affecting the material can be attributed to these factors and to the use of firing temperatures no higher than 850°C.

The compact box morphology and H-shape of the area 4 bricks have hastened certain added weakening to this process. In area 3 bricks that feature the lime-based surface layer identified, its textural difference with the underlying clay also induce a substantial plane of weakness at the interface between the two materials, favouring their separation and the detachment of the former. Nevertheless, the bricks in area 3 are better conserved and their surfaces less decayed than the material in the other three areas, especially those located at lower courses. The shorter time that these bricks have been in place and the protection afforded them by the upper fourth-storey parapet must also be taken into consideration in this respect, however. The colour variations observed, particularly in bricks in which the stretchers are in contact with the openings (framed with stone in the main body and unframed in the setback attic) and in corner bricks,

would indicate that the concern for quality was confined to the headers only, i.e., the surfaces expected to be exposed.

Other factors that would favour the differential decay observed in bricks with similar dimensions and positions or exposed, in principle, to the same agents of alteration, must also be borne in mind, such as firing time or other non-uniform kiln conditions.

#### 4.3. Recommendations for preventive conservation

The parapet crowning the façades is in need of repair, following on a visual inspection of the surfaces of all the bricks to stabilise any at risk of detachment. Where detachment is deemed to be most significant, the inner parapet brickwork should be inspected to determine the possible existence of construction factors that may be favouring the concentration of moisture.

If new bricks are manufactured to replace material in the upper parapet, the existing surfaces should first be cleaned and repaired and the new bricks fired at temperatures of over 900°C. The new units should exhibit a yellowish hue similar to the colour of most of the bricks in this area to minimise possible façade colour changes. To that end, colour coordinate  $a^*$  values should range from 10 to 12.5 and  $b^*$  values from 22 to 28. Similarly, the  $L^*$  value should lie between 57 and 63 and the  $C^*$  value between 24 and 30.

At the very least, the capping that seals the upper parapet on the setback attic should be cantilevered further outward and a dripstone should be carved to minimise the impact of rainwater on surfaces of bricks located beneath.

#### 4.4. Final conclusion

In light of the volume and complexity of the project, the façade design and the ceramic materials used were manufactured prioritising construction functionality at the lowest possible cost. Brick manufacture was not immune to the budget cuts that must have informed construction throughout. Given the enormous number of units needed, any factor that lowered costs constituted an indisputable advantage. Foremost among such factors were the type of clay used and the manufacturing technology employed.

The differential decay exhibited by the bricks is indicative of the different stages of deterioration that affect the exposed surfaces over time. A variety of factors conditions ceramic materials decay in historic buildings, including manufacturing procedures and position on façades. Insufficient protection is one of the primary causes of façade brick decay.

### **Acknowledgements**

The authors wish to thank Antonio Letón, head architect, UCM Works Division, for the support and assistance provided. The support provided by Mariam Barajas, Petrology and Geochemistry Department, Faculty of Geology (UCM); Iván Serrano, Geosciences Institute Microscopy and Mineralogy Unit; Xavier Alonso, Geological Techniques Research Support Centre, Faculty of Geology (UCM); and Antonio Tomás, Electron Microscopy Facility, National Centre for Metallurgical Research (CENIM), Spanish National

Research Council (CSIC) is also gratefully acknowledged. This research was funded under the Geomateriales 2 Programme (S2013/MIT\_2914) and by the UCM research group "Alteration and conservation of Heritage stone materials" (ref. 921359). Finally, thanks are given to the professional support provided by the TechnoHeritage network of Science and Technology for the Conservation of Cultural Heritage.

## References

Adell, JM., 1992. 19th century brick architecture: rationality and modernity. *Informes de la Construcción* 55(521), 5-15.

Aly, N., Gomez-Heras, M., Hamed, A., Alvarez de Buergo, M., Soliman, F., 2015. The influence of temperature in a capillary imbibition salt weathering simulation test on Mokkattam limestone. *Mater. Construcc.* 65(317), e044.

Archivo General UCM, caja ES\_AGUCM\_AH-0270, serie ES, AGUCM, UCM, 06.0.04. Expedientes de concursos de obras. Junta Constructora de la Ciudad Universitaria. 1928 / 2008 - Papel. Archivo General de la UCM.

Archivo General de la UCM (caja ES\_AGUCM\_AH-0176, serie - ES, AGUCM, UCM, 06.0.06). Obras de construcción de la Facultad de Medicina. Empresa adjudicataria. Junta Constructora de la Ciudad Universitaria. 1931 / 1935 - Papel. Archivo General de la UCM.

Campbell, JWP., Price, W., 2005. *Ladrillos, Historia Universal*. Ed. Blume, Barcelona

Carretero, M.I., Dondi, M., Fabbri, B., Raimondo, M., 2002. The influence of shaping and firing technology on ceramic properties of calcareous and noncalcareous illitic-chloritic clays. *Appl. Clay Sci.* 20, 301-306.

Commission Internationale de l'Eclairage, 1978. CIE Recommendations on uniform color spaces, color-difference equations and psychometric color terms. *Colorimetry*, supplement, 2-15.

Cultrone, G., Rodriguez-Navarro, C., Sebastian, E., Cazalla, O., de la Torre, M.J., 2001. Carbonate and silicate phase reactions during ceramic firing. *Eur. J. Mineral.* 13, 621-635.

Cultrone, G., Sebastian, E., Huertas, M.O., 2007. Durability of masonry systems: a laboratory study. *Constr. Build. Mater.* 21(1), 50-51.

Cuomo di Caprio, N., Vaughan, S.J., 1993. An experimental study in distinguishing grog (chamotte) from argillaceous inclusions in ceramic thin sections. *Archeomaterials* 7, 21-40.

Chías, P., 1986. *La Ciudad Universitaria de Madrid. Génesis y Realización*. Ed. Universidad Complutense de Madrid

- Fort, R., Bernabeú, A., García del Cura, M.A., López de Azcona, M.C., Ordóñez, S., Mingarro, F., 2002. Novelda Stone: a stone widely used within the spanish architectural heritage. *Mater. Construcc.* 52(266), 19-32.
- Fort, R., Alvarez de Buergo, M., López de Azcona, M.C., Mingarro, F., Varas, M.J., Soriano, J., 2004. Caracterización de la Fábrica de Ladrillo del Palacio del Infante Don Luis, Boadilla del Monte, Madrid. *Bol. Soc. Esp. Ceram.* V. 43(2), 578-582.
- Fort, R., Alvarez de Buergo, M., Perez-Monserrat, E.M., Gomez-Heras, M., Varas-Muriel, M.J., Freire, D., 2013. Evolution in the use of natural building stone in Madrid, Spain. *Q.J. Eng. Geol. Hydroge.* 56, 521-529.
- Freire-Lista, D.M., Fort, R. The Piedra Berroqueña Region: Candidacy for Global Heritage Stone Province Status. *Geosci. Can.* (in press).
- Friedman, G.M., 1959. Identification of carbonate minerals by staining methods. *J. Sediment. Petrol.* 29, 87-97.
- Galán-Arboledas, R.J., Merino, A., Bueno, S., 2013. Utilización de nuevas materias primas y residuos industriales para mejorar las posibilidades de uso de los materiales cerámicos del área de Bailén (Jaén). *Mater. Construcc.* 63(312), 553-568.
- Gomez-Heras, M., López-González, L., García-Morales, S., Fort, R., Alvarez de Buergo, M., 2014. Integrating non-destructive techniques with photogrammetry 3D models for the development of Geographic Information Systems in heritage structures. In: Rogerio-Candelera, M.A. (Ed), *Science, Technology and Cultural Heritage*. Taylor & Francis Group, London, pp. 429-434.
- González, I., Galán, E., Miras, A., Aparicio, P., 1998. New uses for brick-making clay materials from the Bailén area (southern Spain). *Clay Miner.* 33(3), 553-565.
- Kingery, W.D., Bowen, H.K., Uhlmann, D.R., 1976. *Introduction to Ceramics*. 2nd ed. New York, John Wiley.
- Kreimeyer, R., 1987. Some notes on the firing colour of clay bricks. *Appl. Clay Sci.* 2(2), 175-183.
- López-Arce, P., Zornoza-Indart, A., Gomez-Villalba, L., Perez-Monserrat, E.M., Alvarez de Buergo, M., Vivar, G., Fort, R., 2013. Archaeological ceramic amphorae from underwater marine environments: Influence of firing temperature on salt crystallization decay. *J. Eur. Ceram. Soc.* 33, 2031-2042.
- Maggetti, M., 1982. Phase analysis and its significance for technology and origin. In: Olin, J.S. (Ed), *Archaeological Ceramics*. Smithsonian Institution Press, Washington D.C., pp. 121-133.
- Maniatis, Y., Simopoulos, A., Kostikas, A., 1981. Mössbauer Study of the Effect of Calcium Content on Iron Oxide Transformations in Fired Clays. *J. Am. Ceram. Soc.* 65(5), 263-269.

Maritan, L., Nodari, L., Mazzoli, C., Milano, A., Russo, U., 2006. Influence of firing conditions on ceramic products: Experimental study on clay rich in organic matter. *Appl. Clay Sci.* 31, 1-15.

Melgarejo, J.C., 2003. Atlas de asociaciones minerales en lámina delgada (Tomo I), Barcelona.

Nodari, L., Marcuz, E., Maritan, L., Mazzoli, C., Russo, U., 2007. Hematite nucleation and growth in the firing of carbonate-rich clay for pottery production. *J. Eur. Ceram. Soc.* 27, 4665-4673.

Perez-Monserrat, E.M., Alvarez de Buergo, M., Gomez-Heras, M., Varas-Muriel, M.J., Fort, R., 2013a. An urban geomonumental route focusing on the petrological and decay features of traditional building stones used in Madrid, Spain. *Environ. Earth. Sci.* 69, 1071-1085.

Perez-Monserrat, E.M., Fort, R., Lopez-Arce, P., Alvarez de Buergo, M., Varas-Muriel, M.J., 2013b. Contribution of analytical techniques to determine the technologies used in the ceramic materials from the Former Workers Hospital of Maudes, Madrid (Spain). *J. Eur. Ceram. Soc.* 33, 579-591.

Peters, T., Iberg, R. 1978. Mineralogical changes during firing of calcium-rich bricks clays. *Am. Ceram. Soc. Bull.* 57(5), 503-509.

Puche, O., Mazadiego, L.F., 2002. Industrias cerámicas históricas de Madrid: hornos continuos y sus chimeneas. In: *Congreso Internacional sobre Património Geológico e Minero*, pp. 391-398.

Rodríguez, A., 2007. Aplicación de los aparejos en las fachadas de fábrica vista de Madrid durante la primera mitad del siglo XX desde la configuración constructiva del muro y la influencia de la coordinación dimensional de la pieza. In: *Jornada Nacional de Investigación en edificación*.

Shoval, S., Gaft, M., Beck, P., Kirsh, Y., 1993. Thermal behaviour of limestone and monocrystalline calcite tempers during firing and their use in ancient vessels. *J. Thermal. Anal.* 40, 263-273.

Shoval, S., Yofe, O., Nathan, Y., 2003. Distinguishing between natural and recarbonated calcite in oil shale ashes. *J. Therm. Anal. Calorim.* 71, 883-892.

Trindade, M.J., Dias, M.I., Coroado, J., Rocha, F., 2009. Mineralogical transformations of calcareous rich clays with firing: A comparative study between calcite and dolomite rich clays from Algarve, Portugal. *Appl. Clay Sci.* 52, 355-355.

Vázquez, M., Jiménez-Millán, J., 2005. Materias primas ricas en arcilla de las Capas Rojas Triásicas (Norte de Jaén, España) para fabricar materiales cerámicos de construcción. *Mater. Construcc.* 55(273), 5-20.

VVAA., 2003. Arquitectura de Madrid, Tomo 2 (Ensanches). Ed. Fundación COAM, Madrid



## Figure and table captions

Figure 1. Overview of the buildings that comprise the Medical Ensemble of the current Complutense University of Madrid (Spain) ca 1935.

Figure 2. Faculty of Medicine façade design.

a) three main components (from bottom up): socle, main body (4 storeys) and setback attic with terrace. b) detail of setback attic: the narrow ledge capping the upper parapet and the cantilevered cornice-like impost, fitted with a dripstone, can be shown.

Figure 3. Areas selected on the façades for in-situ measurements (areas 1, 2 and 3) or sampling (areas 1, 2, 3 and 4). Details showing the 39 bricks measured (numbered from 1 to 39, in yellow) and the samples taken (No.1 to No.13, in blue, red or green), mostly from the same 39 bricks.

Figure 4. Location of the Spanish provinces of Madrid and Jaén and geological map of Bailén surrounding area.

Clay materials used to manufacture the bricks analysed: Miocene marl clays underlying the town of Bailén and surrounds and red Triassic clays found around Linares and Guarromán (MAGNAS, Nos. 885 and 905).

Figure 5. Brick bonds and appearance (colour and texture).

a) thin bricks in main body façade enclosures: (1) yellowish and smooth surfaces; (2) dark yellow and rough; (3) dark brown; (4) yellowish, partly reddish, smooth; (5) off-white or light grey and smooth surface. b) brickwork on upper attic parapet: joint mortar pointing on the inside as well as the lower cantilevered cornice and the non-cantilevered capping can be shown. c) dry-jointed brick in setback attic: the very smooth and uniform yellowish surface on some of the bricks is displayed.

Areas 1, 2 and 3: surface hue and texture of some of the bricks selected for in-situ measurements and sampling (numbering and colour code as in Figure 3).

Figure 6. Main forms of decay observed in façade bricks.

a) gradual colour change and increasing roughness in bricks that interface with the stone framing on openings. b) gradual change in surface texture in corner bricks (setback attic). c) partial detachment of bricks in the upper brickwork parapet on the setback attic due to the scant protection afforded by the capping, compared to the bricks under and protected by the cantilevered impost.

Figure 7. Colour coordinate  $a^*$  versus coordinate  $b^*$  for the 39 bricks analysed, grouped by hue [group A (off-white, pale grey), group B (yellowish), group C (reddish-brown)] and showing smooth/rough surface texture and area number as well as the mean  $L^*$ ,  $a^*$ ,  $b^*$  and  $C^*$  values and standard deviations for each colour group.

Figure 8. Samples from four areas on the façades and respective thin sections.

Figure 9. Polarised optical micrographs of the bricks studied. Crossed nicols in 9e, parallel nicols in rest; Q=quartz; GF=granite fragment.

Figure 10. Diffractograms derived from the samples analysed.

Figure 11. FESEM-EDS microstructure, microtexture and elemental composition of sample No.9 from area 3 (setback attic): a) BSE images; b), c) and d) SE images.

Table 1. Brick sampling and in-situ and laboratory characterisation.

- (1) Numbering as in yellow in Figure 3 for areas 1, 2 and 3 (bricks 1-39).
- (2) Samples taken from pieces with hue similar to the colour of the bricks measured in situ (No.1-No.13).

Table 2. Dimensions, mean and standard deviation surface moisture and colour parameters measured in situ bricks (1-39).

Mean surface moisture and standard deviation for the bricks in each area and mean moisture and colour values by rough or smooth surface texture are also pointed out.

- (1) Numbering as in yellow in Figure 3 for areas 1, 2 and 3.

\*Outlier (header range 139 to 144 mm must be taken into account)